

## Assessment of pressure-time-based wave impact criteria from a structural response perspective: application to green water loads



Gang Nam Lee<sup>1</sup> and Kwang Hyo Jung<sup>2,\*</sup>

<sup>1</sup>Department of Ocean System Engineering, Jeju National University, Korea

<sup>2</sup>Department of Naval Architecture and Ocean Engineering, Pusan National University, Korea

### ARTICLE INFO

#### Keywords:

Wave impact  
Green water  
Strain rate  
Impulsiveness

### ABSTRACT

Wave impact loads, such as green water loading, are a critical concern for the structural safety of ships operating in severe sea conditions. Wave impact loads are commonly described as loads that increase rapidly over a short time; however, the criteria used to define wave impact loading differ between hydrodynamic descriptions and structural response considerations, and the connection between these two viewpoints remains unclear. To address this limitation, the present study investigates wave impact loading from a structural response perspective, with a focus on the roles of load impulse and loading rate. A simplified single-degree-of-freedom (SDOF) model, representing the local bending behavior of hull plating, is used to evaluate displacement and strain rate responses under idealized wave impact loading. The results indicate that displacement is mainly governed by load impulse, whereas strain rate response is strongly affected by the rate of load application. Even for wave impact loads with the same impulse, short-duration loading induces pronounced dynamic responses with high strain rates, while longer-duration loading results in quasi-static-like behavior. Based on these findings, a loading-rate-based impact index,  $I_p$ , is applied to green water loading and interpreted from a structural response perspective. Analysis of measured green water pressures shows that impact-type and quasi-static loads can be distinguished at approximately  $I_p \approx 500$ , which is proposed as a practical threshold for classifying wave impact loading.

### 1. Introduction

Ships and offshore structures are continuously exposed to waves during operation, and various types of wave loads act on hull plating and deck structures [1]. Ordinary wave loads can generally be treated as quasi-static loads with relatively smooth time variation; however, under severe sea conditions, wave impact loads may occur, in which large pressures are applied to the structure over a very short duration. Such wave impact loads act on highly localized regions and differ fundamentally from ordinary wave loads in terms of structural response time scale and damage mechanism [2].

\* Corresponding author.

E-mail address: [kjung@pusan.ac.kr](mailto:kjung@pusan.ac.kr)

Among various wave impact phenomena, green water refers to the overtopping of seawater onto the bow or along the flare surface, which directly impacts the deck and superstructure and generates repetitive, localized impact loads. Previous measurements and experimental studies have shown that green water loads exhibit complex pressure–time histories, consisting of an impulsive component with a rapid pressure rise and a quasi-static component with a longer duration [3]. Moreover, the characteristics of these loads strongly depend on the impact location (weather side or deck) and hull geometry, particularly the flare angle [4].

Compared with ordinary wave loads, wave impact loads—such as those generated by green water and other fluid–structure collision phenomena—transfer a large amount of load to the structure within a very short time. Such loading characteristics may lead to local structural damage, vibration excitation, and a reduction in fatigue life. For this reason, evaluating wave loads solely based on their pressure magnitude is insufficient, and the need for clear criteria to determine which loads should be regarded as structural impact loads has been repeatedly emphasized in the literature [5]. In particular, because impact and quasi-static loads differ not only in pressure magnitude but also in loading duration and time-history shape, their resulting structural responses can be fundamentally different, making quantitative classification criteria essential for structural design and safety assessment.

Efforts to establish criteria for identifying wave impact loads have primarily originated from a hydrodynamic perspective. In this context, impact loads are commonly defined as high-pressure loads acting over a short duration [6], and classical hydrodynamic theories, such as Wagner theory [7], have been used to explain pressure amplification during fluid–structure impact based on momentum change and the rapid expansion of the contact region. Subsequent experimental studies have therefore focused on peak pressure and pressure rise time as key descriptors of impact loading [8, 9].

Based on these descriptors, Allsop et al. [10] classified wave loads on vertical walls into impulsive (or dynamic) loads and pulsating loads with relatively long duration, while Oumeraci et al. [5] further proposed a dynamic classification framework considering pressure time-history shape and generation mechanism. Although these classifications are useful for understanding wave loads on vertical structures, their applicability is limited to specific geometries and becomes less robust when pressure time histories vary significantly. To address this limitation, Ariyaratne et al. [11] and Lee et al. [4] proposed loading-rate-based impact indices, such as impulsiveness ( $I_p$ ), that simultaneously account for pressure magnitude and rise time and applied them to distinguish impact and quasi-static loads in green water and wave-impact experiments.

From a structural dynamics perspective, impact loading is classified based on structural response criteria, with particular emphasis on the time scale of loading relative to the structural natural period. In particular, structural response depends strongly on whether the load duration is long or short relative to the structural natural period, leading to fundamentally different response mechanisms [12, 13]. When the load duration is much longer than the natural period, the response approaches quasi-static behavior. In contrast, very short-duration loading acts as a sudden acceleration input, resulting in pronounced dynamic response and high strain rates [12, 14].

Based on this concept, NORSOK Standard [15] and International Ships and Offshore Structure Congress (ISSC) [16] proposed classifying loads into quasi-static, dynamic impact, and impulsive impact categories using the ratio of impact duration to structural natural period. By contrast, Hayashi and Tanaka [17] classified loads into creep, static, dynamic, impact, and ultra-high-rate impact based on the strain-rate-associated with the loading rate. However, these response-based classification schemes do not necessarily coincide with the commonly used notion of wave impact loads defined by a rapid pressure rise and may therefore be conceptually distant from impact definitions based solely on hydrodynamic loading characteristics.

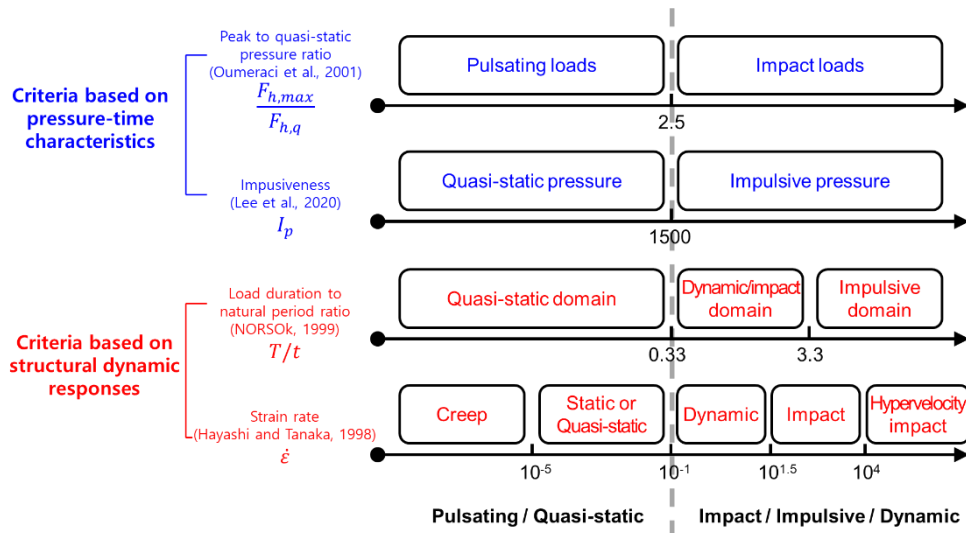


**Fig. 1** Schematic comparison of fluid-dynamics based and structural response-based criteria for wave impact loads

Figure 1 conceptually illustrates representative impact load classification criteria previously proposed from hydrodynamic considerations and from structural response. Hydrodynamic approaches primarily characterize wave impact loads using pressure–time features, such as peak pressure, rise time, and impulse, which are effective for describing the characteristics of the fluid loading itself but are not directly linked to structural response. In contrast, structural response-based approaches focus on temporal loading characteristics, including load duration relative to the structural natural period and strain rate, highlighting the importance of time scale in governing structural behavior. While these criteria provide clear insight into structural response mechanisms, they remain difficult to apply directly to pressure time histories measured in real wave impact events.

As discussed above, existing criteria for classifying wave impact loads have been developed predominantly from either hydrodynamic description of pressure–time characteristics or structural response considerations based on structural time scales. While structural dynamics theory clearly indicates that short-duration loading leads to acceleration-dominated response and elevated strain rates, such criteria are typically formulated using structural parameters such as natural period and damping ratio, which are not directly available when impact loads are assessed solely from measured or simulated pressure histories. From a practical design and assessment perspective, however, impact-type wave loads must often be identified prior to detailed structural analysis, based only on the characteristics of the applied fluid loads. This creates a gap between response-based impact definitions and pressure-based load descriptions commonly obtained from experiments and numerical simulations.

To address this gap, the present study proposes an analytical approach that links pressure–time characteristics of wave impact loads, with particular emphasis on green water loading, to structural response. A simplified structural model representing the local bending behavior of ship hull plating is employed to examine the influence of key temporal loading parameters, including loading duration and loading rate, on deformation and strain rate response. Rather than predicting structural failure, this study aims to identify the loading characteristics governing strain-rate-dominated response under wave impact loading and to provide a structural response-based interpretation of existing loading-rate-based impact descriptors for practical green water events.

## 2. Structural model and governing equations

### 2.1 Simplified structural model for hull plating

To investigate the structural response characteristics associated with wave impact loading, the present study considers a simplified structural model that represents the local behavior of ship hull plating. Rather than modeling the global response of an entire ship structure, the focus is placed on local plate bending, which

is widely recognized as the dominant response mode under short-duration impact loading. Such simplified plate models have been commonly adopted in previous studies to capture the essential dynamic response of hull plating subjected to wave and impact loads [18-21].

Following this approach, the structural response is evaluated using a fully clamped square plate model, which provides a representative and well-established idealization for hull plating supported by surrounding stiffeners. Dry structural modes are adopted since the transient nature of impact loading makes the definition of wet modes difficult. This modeling framework enables a clear and systematic examination of the influence of temporal loading characteristics, such as loading rate and impulse, on deformation and strain rate response, while avoiding additional complexities associated with global structural behavior. The main geometry in this study is shown in Figure 2, while corresponding material properties and geometric parameters are summarized in Table 1.

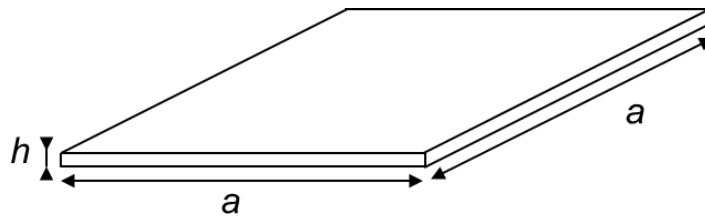


**Fig. 2** Simplified structural model for hull plating

**Table 1** Dimensions and material properties of hull plating model

Properties	Value
Yield strength ( $\sigma_0$ )	247 MPa
Density ( $\rho$ )	7,850 kg/m <sup>3</sup>
Poisson ratio ( $\nu$ )	0.303
Young's modulus ( $E$ )	210 GPa
Length ( $a$ )	900 mm
Thickness ( $h$ )	9 mm

## 2.2 Governing equations for structural analysis

In order to quantitatively investigate the influence of wave impact load characteristics on structural response, a structural dynamic analysis is conducted using the simplified hull plating model introduced in the previous section. The analysis focuses on capturing the dominant response mechanisms induced by impact loading, rather than reproducing detailed local stress distributions or damage states of a specific ship structure. To this end, the local bending behavior of the hull plate element is idealized as a single-degree-of-freedom (SDOF) structural dynamic system. The plate is represented as an equivalent mass–spring–damper system, and the governing equation of motion is expressed as:

$$m\ddot{u}(t) + c\dot{u}(t) + ku(t) = F(t) \quad (1)$$

where  $u(t)$  is the equivalent displacement representing the first bending mode of the hull plate element, serving as a representative modal coordinate rather than a specific local displacement. And  $\dot{u}(t)$  and  $\ddot{u}(t)$  denote the corresponding velocity and acceleration, respectively. The equation of motion was solved by time-domain numerical integration using the measured pressure history as the external force. A time-marching scheme based on explicit Euler velocity update and semi-implicit displacement update was adopted.

The parameters  $m$ ,  $c$ , and  $k$  are the equivalent mass, damping coefficient, and equivalent stiffness of the SDOF system. The external force ( $F(t)$ ) represents the equivalent force acting on the plate due to impact loading and is obtained by spatially integrating the time-varying pressure over the plate area.

In the present study, stiffness  $k$  is defined so that the natural frequency of the SDOF system matches the first natural frequency of a fully clamped square plate. Accordingly, stiffness is determined as:

$$k = (2\pi f_1)^2 m \quad (2)$$

where  $m$  is taken as the total mass of the plate as a simplified representation of the modal mass associated with the first bending mode, since the objective is to examine the relative influence of load impulse and loading rate rather than absolute response levels.

Accordingly, the natural circular frequency of the SDOF system is given as:

$$\omega_n = \sqrt{\frac{k}{m}} = 2\pi f_1 \quad (3)$$

The first natural frequency  $f_1$  of the plate can be obtained from Equation (4).

$$f_1 = \beta^2 \sqrt{\frac{D}{\rho h a^4}} \quad (4)$$

where  $a$  is the plate side length and  $\beta$  is the mode coefficient determined by the boundary condition. In this study, a value of  $\beta=35.99$  is adopted for a fully clamped square plate [22]. The bending stiffness ( $D$ ) of the plate is calculated as:

$$D = \frac{Eh^3}{12(1-\nu^2)} \quad (5)$$

The damping coefficient ( $c$ ) is defined assuming a viscous damping model as Equation (5).

$$c = 2\zeta\sqrt{km} \quad (6)$$

where  $\zeta$  is the damping ratio. In this study, the value of  $\zeta=0.02$  is used, which is commonly adopted for the dynamic response of steel hull plating structures [14].

It is emphasized that the present SDOF model is not intended to predict absolute stress or strain levels of a specific structural configuration. Rather, it is adopted to examine the relative sensitivity of structural response characteristics to variations in load impulse and loading rate, which constitute the primary focus of the present study. Within this context, the simplified representation is sufficient to capture the dominant response trends associated with short-duration wave impact loading.

### 3. Characterization and simplification of impact loads

#### 3.1 Target impact loads

In the present study, green water loading is adopted as a representative form of wave impact loading, as it exhibits a wide range of pressure magnitudes and temporal characteristics under severe sea conditions. The impact load characteristics considered in this study are defined based on green water pressure measurements reported by Lee et al. [3, 4, 23], obtained from experiments conducted in a two-dimensional wave flume using a simplified fixed structure at a scale of 1:125. The experiments employed a rectangular structural model instrumented with pressure sensors distributed along the structural surface, as shown in Figure 3. The measurements include both slamming-type wave loads acting on the weather side of the structure and overtopping-induced loads associated with water running onto the deck and impacting the structural surface.

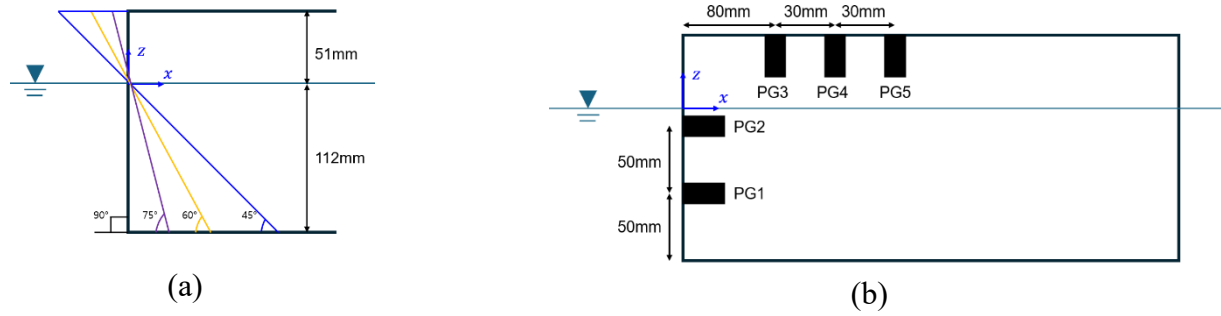


**Fig. 3** Definition of flare angle and location of pressure sensors for measurement of green water loading under wave height of  $H_{1/100}$  (redrawn based on Lee et al. [3])

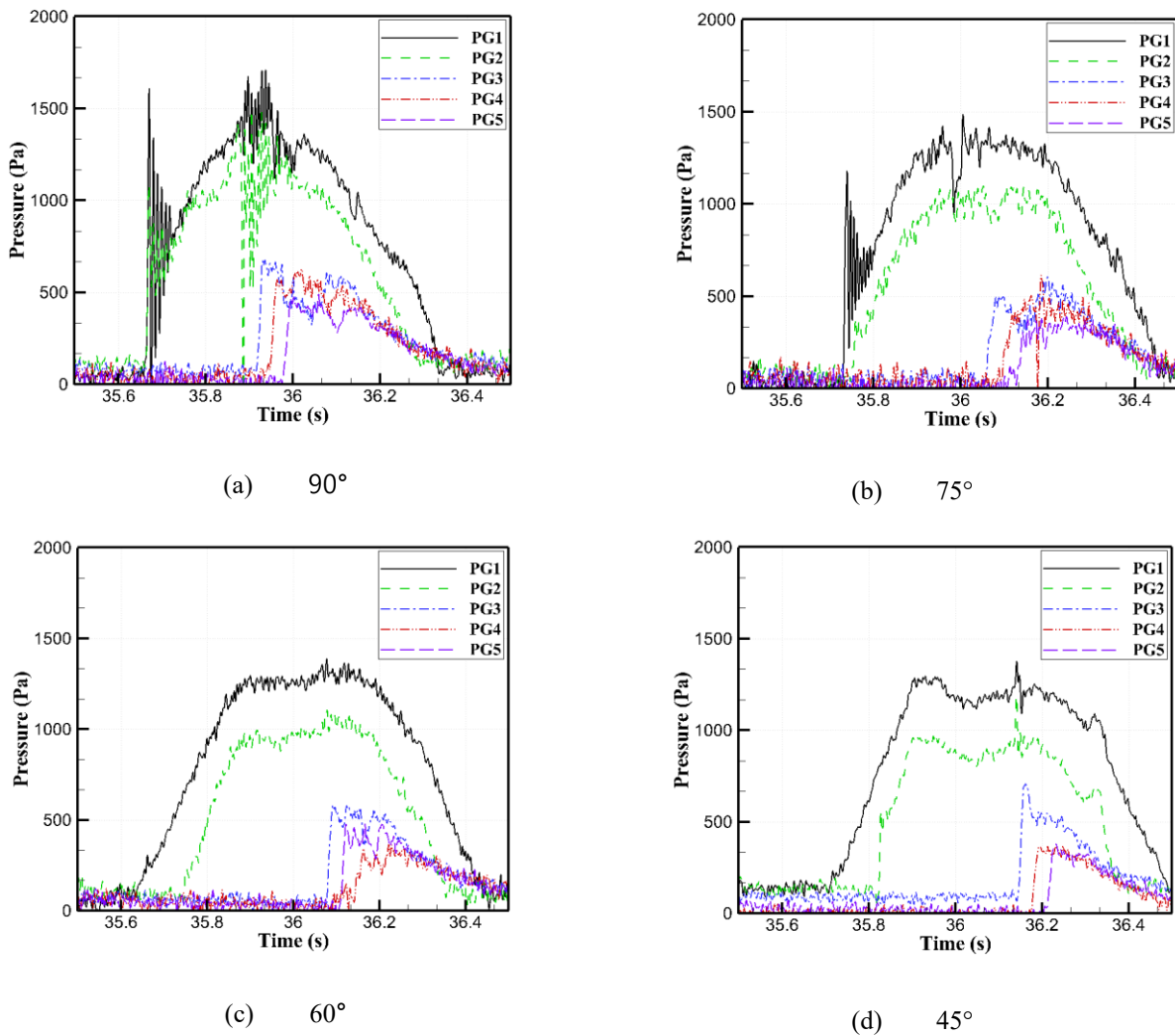


**Fig. 4** Pressure distributions of green water for various flare angles under wave condition of  $H_{1/100}$  (redrawn based on Lee et al. [4])

The measurements reported by Lee et al. [4] indicate that the temporal characteristics of green water pressure loads vary significantly depending on the flare angle and measurement location. In particular, both impulsive pressure loads characterized by a sharp and sudden rise and quasi-static pressure loads with a more gradual increase and longer duration were observed, as illustrated in Figure 4. The pressure histories shown in Figure 4 are replotted from experimental data reported in the Lee et al. [4]. For relatively large flare angles ( $90^\circ$  and  $75^\circ$ ), pronounced impulsive pressure peaks were recorded on the weather side of the structure, whereas pressure histories measured on the deck side exhibited smoother temporal variation, indicating the quasi-static-dominated behavior. In contrast, for smaller flare angles ( $60^\circ$  and  $45^\circ$ ), impulsive pressure peaks

were not clearly observed even on the weather-side, while the deck-side pressure characteristics remained similar across all flare angles.

Based on these observations, the present study focuses on pressure time histories measured at a flare angle of  $90^\circ$ , where the distinction between impulsive and quasi-static characteristics is most evident. Pressure records obtained under the representative wave conditions of  $H_{1/3}$ ,  $H_{1/10}$ , and  $H_{1/100}$  are considered. In addition, pressure histories measured under the  $H_{1/100}$  wave condition for flare angles of  $45^\circ$ ,  $60^\circ$ ,  $75^\circ$ , and  $90^\circ$  are included to examine the influence of flare angle on impact load characteristics. The rise and decay times from Lee et al. [4] are defined using the half-peak method, as illustrated in Figure 5. For the evaluation of loading-rate characteristics, the analysis focuses on the initial rapid pressure-rise portion of the measured pressure histories.

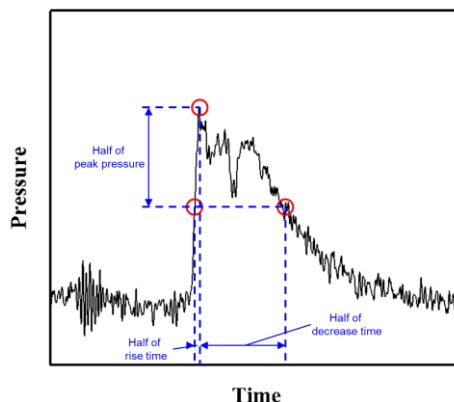


Fig. 5 Definition of peak pressure, rise time, and decay time using the half-peak method

### 3.2 Scaling of impact loads

To evaluate the structural response using green water pressure measurements obtained from model-scale experiments, an appropriate scaling procedure is required. Wave loads acting on ships and offshore structures are commonly scaled based on geometric similarity and Froude similarity, which generally provide reasonable results for gravity-dominated phenomena. However, wave impact loads, such as green water impact, are characterized by a rapid pressure rise over a very short duration and involve physical processes that cannot be fully captured by Froude similarity alone [24].

In particular, wave impact events are frequently accompanied by air entrainment in front of the structure, leading to the formation of an air layer whose compressibility and density differ significantly from those of water. This entrapped air layer influences the pressure transmission mechanism during impact and affects both the magnitude and temporal characteristics of the resulting pressure history [4, 25, 26]. Accordingly, direct conversion of model-scale impact pressures to full scale using conventional Froude scaling may result in an over-estimation of the actual impact pressure.

To account for these effects and obtain a more realistic estimation of full-scale impact pressures, the present study adopts a scaling approach based on the Bagnold number, which was originally proposed for wave impact problems on vertical walls [25]. The Bagnold number ( $Bgn$ ) is a dimensionless parameter that characterizes the interaction between the entrapped air layer and the water body during wave impact and is defined as follows [27]:

$$Bgn = \frac{\rho_w k_w u_{max}^2}{p_0 t_a} \quad (7)$$

where  $\rho_w$  is the water density,  $p_0$  is the atmospheric pressure, and  $u_{max}$  is the maximum horizontal velocity of incoming wave. The parameters  $t_a$  and  $k_w$  represent the characteristic thicknesses of the air layer and the water body, respectively. In the present study, these parameters are estimated using the significant wave height  $H_s$  as:

$$t_a = \pi H_s / 12 \quad (8)$$

$$k_w = 0.2 \left(1 - \frac{\pi}{12}\right) H_s \quad (9)$$

Based on the calculated Bagnold number, the relationship proposed by Cuomo et al. [22] is applied to estimate the maximum impact pressure ( $p_{max,F}$ ) as:

$$Bgn = 5 \left(\frac{p_{max,F}}{p_0}\right)^{2/7} + 2 \left(\frac{p_{max,F}}{p_0}\right)^{-5/7} - 7 \quad (10)$$

Using this relationship, the corrected scale factor for pressure,  $\lambda_s$ , is derived as:

$$\lambda_s = \frac{(p_{max,F} - p_0)/p_0}{(p_{max,M} - p_0)/p_0} \quad (11)$$

where,  $p_{max,M}$  is the maximum impact pressure in model-scale. The same scaling concept is also applied to the rise time of the impact load, and the full-scale rise time is obtained as:

$$t_{r,F} = \frac{\lambda_f^{3/2}}{\lambda_s} t_{r,M} \quad (12)$$

where  $t_{r,F}$  and  $t_{r,M}$  are the rise time for full and model scales, and  $\lambda_f$  is the geometric scale ratio. The Bagnold numbers evaluated at both model and full-scales, together with the corresponding pressure scaling factors, are summarized in Table 2. The resulting scaling factors that account for air entrainment effects are smaller than those obtained using conventional Froude scaling, indicating the pressure attenuation caused by the air-cushion effect during wave impact events [28, 29]. It should be noted that this scaling approach, originally developed for vertical-wall wave impact, is used here as an engineering approximation for structural response analysis and does not fully represent the complex hydrodynamic characteristics of deck green water flow.

**Table 2** Bagnold number and corrected pressure scale factor ( $\lambda_s$ ) for model and prototype cases at flare angles of 90° and 75°

Flare angle (°)	$Bgn_M$	$Bgn_F$	$\lambda_s$
90	0.043	5.359	75.071
75	-	-	54.634

### 3.3 Load simplification

Measured green water pressures typically exhibit highly complex time histories in which a rapidly rising impulsive component is superimposed on a more gradually varying quasi-static component. When such pressure histories are directly applied to structural dynamic analysis, it becomes difficult to clearly distinguish the influence of individual load parameters on the resulting structural response, which is the primary focus of the present study.

To address this issue, an idealized pressure–time history is introduced that retains the essential temporal characteristics of green water impact loading while enabling independent control of representative load parameters. In this study, the maximum pressure ( $p_{max}$ ) and the rise time ( $t_r$ ) are selected as the primary parameters characterizing the impact load. To ensure a smooth pressure variation and to avoid non-physical discontinuities in pressure slope that may induce artificial high-frequency response, a raised-cosine-type pressure history is adopted [30]. The idealized pressure history is defined as follows:

$$P(t) = \begin{cases} \frac{P_{eff}}{2} \left[1 - \cos\left(\frac{\pi t}{t_r}\right)\right], & 0 < t \leq t_r \\ \frac{P_{eff}}{2} \left[1 + \cos\left(\frac{\pi(t - t_r)}{t_d}\right)\right], & t_r < t \leq t_r + t_d \end{cases} \quad (13)$$

where  $P_{eff}$  denotes the effective peak pressure of the idealized raised-cosine load. It is defined such that the simplified pressure history has the same impulse as the reference impact load, as expressed by:

$$P_{eff} = \frac{2I_{ref}}{T} \quad (14)$$

where  $I_{ref}$  is the impulse of the reference pressure and  $T$  is the effective duration of the impact load, defined as the sum of the rise time and decay time. The  $I_{ref}$  is given by:

$$I_{ref} = \int_0^T P dt \quad (15)$$

The  $T$  is defined as:

$$T = t_r + t_d \quad (16)$$

Accordingly, the measured pressure histories are transformed into simplified impact load profiles, as schematically illustrated in Figure 6. The figure compares the measured pressure history with a conventional triangular idealization and the raised-cosine-based pressure history proposed in this study. While the triangular pressure model can approximate the overall duration and peak pressure, it introduces non-physical discontinuities in the pressure slope. In contrast, the raised-cosine model provides a smooth pressure evolution while preserving the impulse and the key temporal characteristics of the measured load. This idealized impact load formulation enables a systematic investigation of the effects of loading rate and impulse on structural response, with particular emphasis on strain rate behavior.

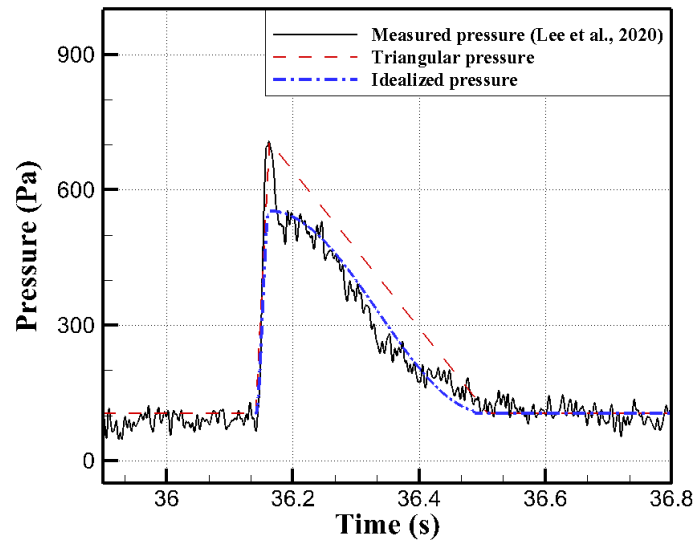
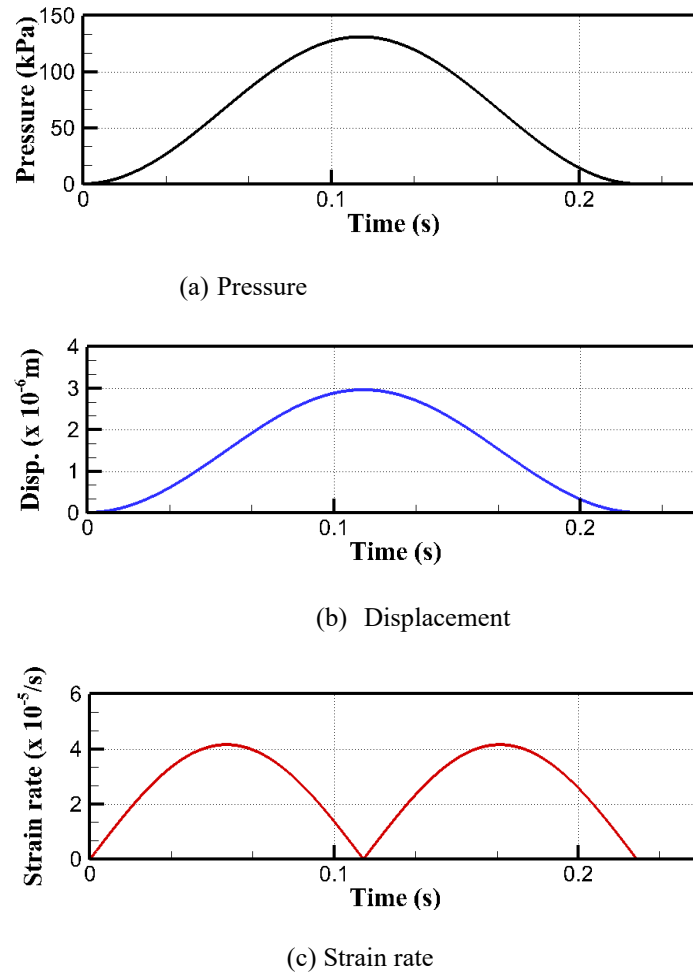


**Fig. 6** Comparison of measured, triangular, and raised-cosine idealized pressure histories

The simplified pressure history adopted in this study is not intended to reproduce individual measured pressure histories in detail. Instead, it is designed to retain the essential temporal characteristics that govern strain-rate-dominated structural response, while eliminating unnecessary complexity inherent in real impact loading. This idealized impact load formulation enables a systematic investigation of the effects of loading rate and impulse on structural response, with particular emphasis on strain rate behavior, although it does not explicitly represent the high-frequency components that may be present in actual wave impact pressure signals. In addition, hydroelastic interaction between structural deformation and fluid loading is not considered in the present analysis.

## 4. Results and discussion

### 4.1 Results of time history of structural responses



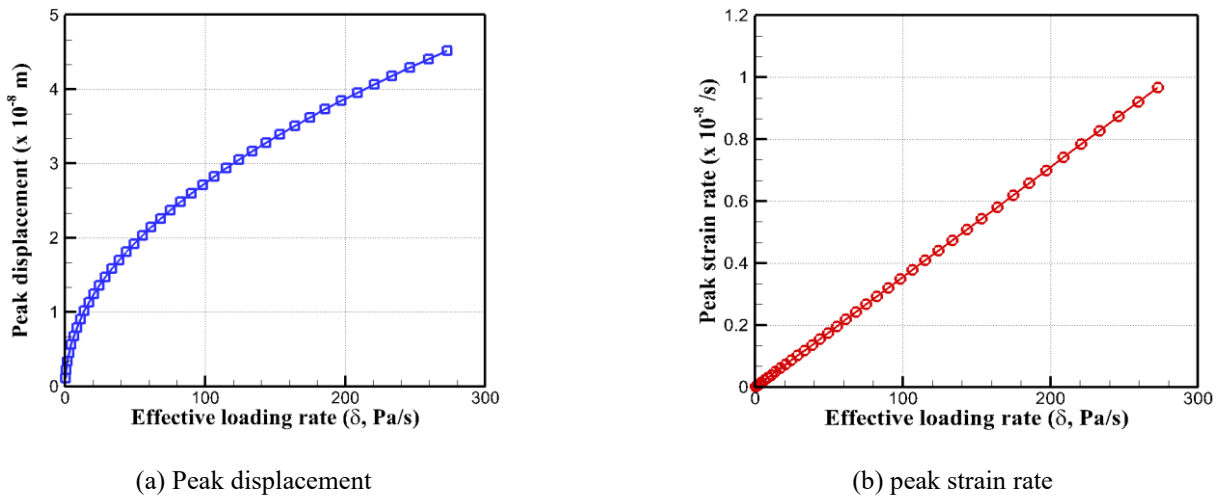
**Fig. 7** Time histories of applied pressure, displacement, and strain rate under impact loading

Figure 7 presents the time histories of displacement (Figure 7(b)) and strain rate responses (Figure 7(c)) of the hull plating structure subjected to the idealized impact load (Figure 7(a)) defined in Section 3.3. The applied load is constructed based on the green water pressure measured by Lee et al. [3] under the  $H_{1/100}$  wave condition, with the measured peak pressure ( $P_{max}$ ) and rise time ( $t_r$ ) adopted. For simplicity, the decay time is assumed to be equal to the rise time ( $t_d = t_r$ ), resulting in a temporally symmetric impact load. The strain rate response is assumed to be proportional to the time derivative of the displacement.

The displacement response exhibits a smooth increase during load application and reaches its maximum near the peak of the applied pressure. The magnitude of displacement is primarily governed by the magnitude and shows limited sensitivity to the detailed temporal variation of the pressure history. In contrast, the strain rate is strongly influenced by the temporal characteristics of the applied load. Pronounced peaks occur during periods of rapid pressure change rather than at the instant of maximum pressure.

For the symmetric impact load considered in Figure 6, in which the rise and decay times are defined to be identical, two distinct peaks naturally appear in the strain rate response during the loading and unloading phases. These peaks indicate that the maximum strain rate is governed by the highest loading rate rather than by the peak load magnitude, highlighting the different load characteristics governing displacement and strain rate responses under wave impact loading.

## 4.2 Effect of loading rate and impulse on structural analysis



**Fig. 8** Effect of loading rate on peak displacement and peak strain rate

Figure 8 presents the variations in peak displacement and peak strain rate responses of the hull plating structure with increasing effective loading rate, while maintaining a constant impulse of the impact load. The effective loading rate ( $\delta$ ) is defined as Equation (17).

$$\delta = \frac{P_{max}}{t_r} \quad (17)$$

The parameter represents the rate at which the impact load is transmitted to the structure. All response quantities are evaluated based on their maximum values attained during the loading event.

In this parametric analysis,  $P_{max}$  is varied from 0 to 2,000 kPa and  $t_r$  from 0.1 to 0.5 s, covering the ranges commonly reported for green water and slamming impact loads in previous experimental studies [31, 32]. While the impulse is kept constant for all loading cases, the selected parameter ranges include both typical and more severe impact conditions to enable a systematic assessment of loading-rate effects. By combining these parameters, a total of 50 loading conditions is considered. The selected ranges of peak pressure and rise time are intended not only to represent typical green water loading conditions, but also to encompass the lower-bound characteristics of slamming-type impact loads reported in previous experimental studies.

The peak displacement response exhibits an increasing trend with increasing effective loading rate; however, the increase becomes progressively less pronounced. This behavior indicates that, under conditions of constant impulse, the displacement response is governed primarily by the overall load magnitude and duration and is relatively insensitive to the detailed temporal concentration of the load. Even when the load is applied over a much shorter duration, the resulting maximum displacement remains within a limited range.

In contrast, the peak strain rate response increases almost linearly with the effective loading rate. This clear dependence indicates that, for impact loads with identical impulse, more rapid load transmission leads to a substantial amplification of deformation rate. The maximum strain rate is therefore governed not by the peak pressure itself, but by the temporal characteristics of the load, particularly the rate at which the pressure is applied.

These results further demonstrate that displacement and strain rate are governed by different characteristics of impact loading, consistent with fundamental structural dynamics considerations. While the displacement response is primarily influenced by impulse related load magnitude and duration, it still exhibits some dependence on the effective loading rate. In contrast, the strain rate response is highly sensitive to the effective loading rate.

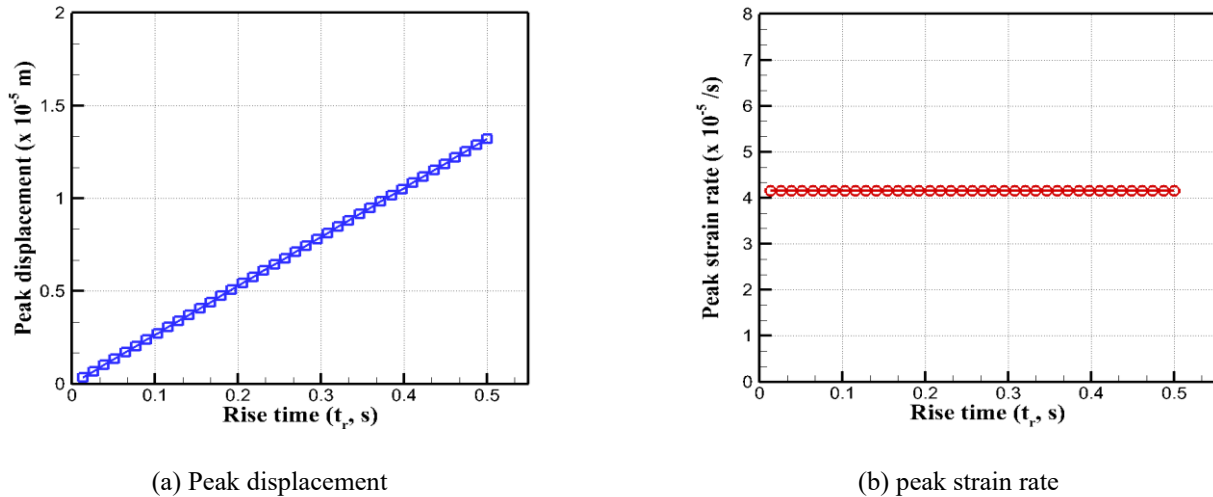


**Fig.9** Effect of impulse on peak displacement and peak strain rate

Figure 9 presents the variations in peak displacement and peak strain rate responses of the hull plating structure as the impulse of the impact load is increased by varying the rise time, while maintaining a constant effective loading rate. The range of rise times and the number of loading conditions are identical to those considered in Figure 8. The decay time is assumed to be equal to the rise time ( $t_d = t_r$ ) and a total of 50 loading conditions are analyzed. As in Figure 7, all response quantities are evaluated based on their maximum values during the loading event.

The peak displacement response exhibits an almost linear increase with increasing rise time. Under conditions of constant effective loading rate, increasing the rise time corresponds to a longer load duration and, consequently, a larger impulse applied to the structure. This trend indicates that the displacement response is primarily influenced by the cumulative effect of the load, represented by the impulse, rather than by the rate at which the load is applied.

In contrast, the peak strain rate response remains nearly unchanged with respect to variations in rise time. When the effective loading rate is held constant, the temporal rate of load transmission to the structure does not vary, even though the load duration and impulse increase. As a result, an increase in impulse does not lead to a noticeable change in the maximum strain rate response.

Taking together with the results shown in Figure 7, these findings indicate that displacement and strain rate are governed by different aspects of impact loading. While displacement is sensitive to changes in load impulse, the strain rate response is controlled primarily by the effective loading rate rather than by the impulse of the applied load.

#### 4.3 Impact load criteria and application to green water loading

The results presented in Sections 4.1 and 4.2 clarify that different temporal characteristics of wave impact loading govern distinct aspects of structural response, with displacement primarily dominated by load impulse and strain rate strongly influenced by loading rate. While this behavior is consistent with general structural dynamics principles, it highlights that displacement- and strain-rate-based responses reflect fundamentally different loading characteristics.

From a structural integrity perspective, this distinction is particularly important because strain rate is closely associated with impact-induced damage mechanisms. High strain rate loading is known to promote localized plastic deformation, coating damage, and crack initiation, even when the associated displacement or stress level remains moderate, and repeated exposure to such events may accelerate fatigue damage accumulation [33]. In this context, the present analysis provides a systematic interpretation of pressure–time characteristics representative of green water loading, with specific emphasis on strain-rate-dominated structural response.

The results presented in Sections 4.1 and 4.2 clarify how different temporal characteristics of wave impact loading influence distinct aspects of structural response. While the observed dependence of displacement on impulse and of strain rate on loading rate is consistent with general structural dynamics principles, the present analysis provides a systematic interpretation of these relationships in the context of pressure–time histories representative of green water loading.

From this perspective, the loading-rate-based impact index  $I_p$ , proposed by Lee et al. [4] from a hydrodynamic viewpoint, can be reinterpreted in terms of strain-rate-dominated structural response. The strong sensitivity of strain rate to loading rate observed in the present analysis provides a physical basis for using  $I_p$  as a practical indicator to distinguish impact-type and quasi-static green water loads based solely on pressure–time characteristics. This interpretation suggests that impact load classification based on loading rate, as embodied in  $I_p$ , is physically meaningful for the structural assessment of green water and wave impact loads, where strain rate effects play a critical role in governing structural response. The  $I_p$  is defined as:

$$I_p = \frac{P_{max}/t_r}{0.5\rho_w u_{max}^2 T_{wave}} \tag{18}$$

where,  $u_{max}$  is maximum horizontal water particle velocity of incoming wave, rather than the deep water wave celerity, and  $T_{wave}$  is wave period.

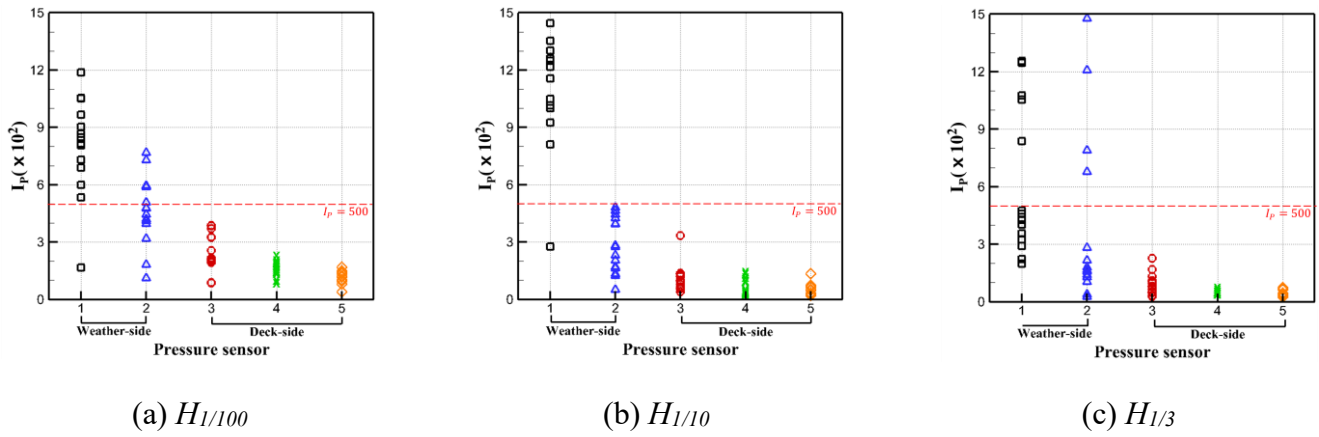


**Fig. 10** Distribution of  $I_p$  for green water pressure measurements at a flare angle of  $90^\circ$  under different wave conditions

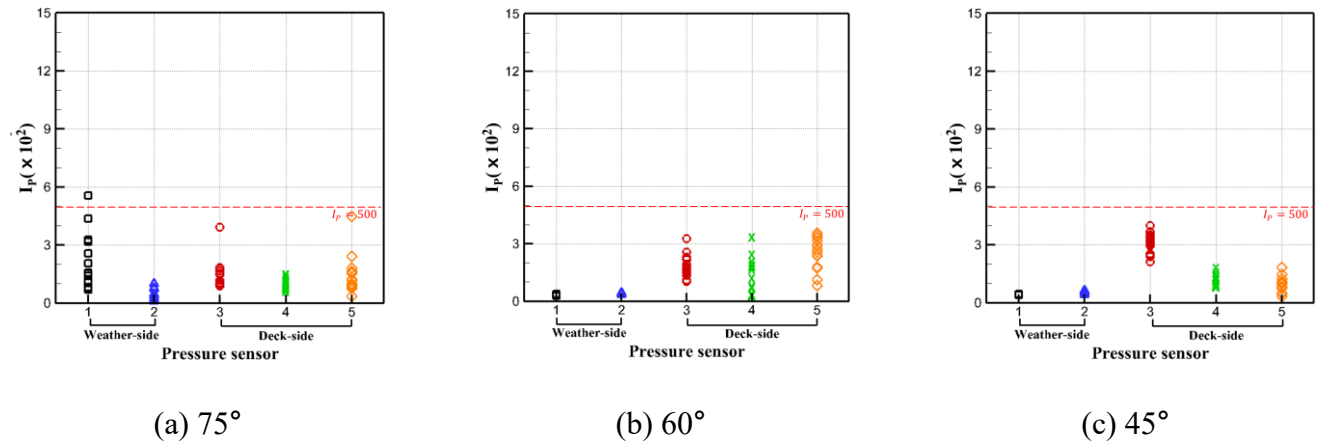


**Fig. 11** Distribution of  $I_p$  for green water pressure measurements under different flare angles at the  $H_{1/100}$  wave condition

Figures 10 and 11 present the distributions of the loading rate-based impact index  $I_p$  evaluated from the green water pressure measurements reported by Lee et al. [3]. Figure 10 shows the results for a flare angle of  $90^\circ$  under different wave conditions ( $H_{1/100}$ ,  $H_{1/10}$  and  $H_{1/3}$ ), while Figure 11 presents the results for varying flare angles ( $75^\circ$ ,  $60^\circ$ , and  $45^\circ$ ) under the  $H_{1/100}$  wave condition. In both figures, sensor locations 1 and 2

correspond to the weather side, whereas sensors 3-5 correspond to the deck side. Each point in the figures represents an individual pressure event obtained from the experimental measurements.

The distributions of  $I_p$  exhibit systematic variations depending on the measurement location, hull geometry, and wave condition. For the flare angle of  $90^\circ$ , relatively large  $I_p$  values are frequently observed on the weather side, whereas  $I_p$  decreases markedly toward the deck-side locations. This indicates that pressure histories measured on the weather side are characterized by short rise times and high-pressure gradients, while deck-side pressures are dominated by more gradual temporal variation. As the flare angle decreases, the overall level of  $I_p$  is reduced, and most values concentrate in a low  $I_p$  range, indicating that green water loads progressively approach quasi-static behavior.

Based on the observed  $I_p$  distributions and the corresponding pressure-history characteristics under the present experimental conditions, the study identifies  $I_p \approx 500$  as a practical threshold for distinguishing impact-type and quasi-static green water loads. This threshold provides a clear separation between the sharp, impulsive pressure histories observed on the weather side and the more gradual pressure histories observed on the deck side and is consistent with the strain-rate-dominated structural response identified in the preceding analysis. Accordingly, loads with  $I_p > 500$  are interpreted as impact-dominated, whereas loads with  $I_p < 500$  exhibit structural characteristics closer to quasi-static loading.

When this threshold is applied to the results in Figures 9 and 10, the impact characteristics of green water loads can be clearly classified according to load location, hull geometry, and wave condition. For a flare angle of  $90^\circ$ , a large proportion of the weather-side measurements fall within the  $I_p > 500$  range for all wave conditions, with both the magnitude and dispersion of  $I_p$  increasing under more severe waves. In contrast, deck-side measurements are predominantly distributed within the  $I_p < 500$  range. As the flare angle decreases to  $75^\circ$ , only a limited number of weather-side measurements exceed the threshold, and for flare angles of  $60^\circ$  and  $45^\circ$ , most measurements fall within the quasi-static range. These results demonstrate that the loading rate-based index  $I_p$  provides an effective and physically meaningful parameter for distinguishing the impact characteristics of green water loads.

It should be noted that the identified threshold value of  $I_p \approx 500$  is not a universal constant, but a reference obtained from the combined effects of structural response characteristics and the temporal properties of the applied wave impact loads. While structural parameters such as plate thickness, boundary condition, and damping ratio may influence the structural response, the threshold value is also affected by the pressure rise-time and loading-rate distributions associated with the impact loads, which depend on wave conditions, hull geometry, and experimental setup. Accordingly, the specific numerical value of the  $I_p$  threshold may vary for different datasets, including both green water and slamming-type impact measurements, whereas the proposed interpretation framework linking loading rate to strain-rate-dominated structural response remains applicable to wave impact loads characterized by short-duration, high loading-rate pressures.

## 5. Conclusions

In this study, the influence of the characteristics of green water impact loads on structural response has been systematically investigated using a simplified structural model. By adopting an SDOF representation of the local bending behavior of hull plating, the relative roles of load impulse and loading rate in governing displacement and strain rate responses were independently examined.

The main findings of this study can be summarized as follows:

1. Displacement response is primarily sensitive to variations in load impulse, whereas strain rate response is governed mainly by the temporal rate at which the load is transmitted to the structure. Even for impact loads with identical impulse, short-duration loading induces pronounced strain rate response, while longer-duration loading leads to structural behavior closer to quasi-static response. These findings highlight the limitation of impulse-based characterization alone for assessing impact severity from a structural response perspective.
2. Within this framework, the loading-rate-based impact index  $I_p$ , originally proposed from a hydrodynamic viewpoint, is reinterpreted in terms of strain-rate-dominated structural response.

3. Analysis of green water pressure measurements reported by Lee et al. [3] indicates that pressure-history characteristics and corresponding structural response tendencies are clearly distinguished around  $I_p \approx 500$  under the present conditions. Accordingly, this value is identified as a practical reference for classifying impact-type and quasi-static green water loads. It should be noted that this threshold value is not a universal constant, but a reference obtained under the specific experimental and structural conditions considered in this study.

The findings of this study provide a structural response-based physical interpretation of existing loading-rate-based impact classification criteria for green water and wave impact loads and offer useful implications for impact load assessment and the development of rational design criteria. Nevertheless, the structural behavior in this study was represented using a simplified SDOF model, and local plastic deformation, cracking, and material nonlinearity were not considered. In addition, the spatial variation of green water pressure along the deck was not explicitly considered, and the applied load was assumed to act uniformly over the representative plate element. Future work should address these limitations through high-fidelity finite element simulations and targeted experimental validation to further establish the applicability and robustness of the proposed impact classification criterion.

## ACKNOWLEDGEMENT

This work was supported by the research grant of Jeju National University in 2025.

## REFERENCES

- [1] Bal, K., Bayraktar Bural, D., 2024. Investigation into forces on offshore piles with constant and linearly varying diameters using CFD and extended Morison equation under separate wave and current loadings. *Brodogradnja*, 75(4), 75406. <https://doi.org/10.21278/brod75406>
- [2] Faltinsen, O., 1993. Sea loads on ships and offshore structures (Vol. 1). *Cambridge university press*. <https://doi.org/10.4043/7142-MS>
- [3] Lee, G. N., Jung, K. H., Malenica, S., Chung, Y. S., Suh, S. B., Kim, M. S., Choi, Y. H., 2020. Experimental study on flow kinematics and pressure distribution of green water on a rectangular structure. *Ocean Engineering*, 195, 106649. <https://doi.org/10.1016/j.oceaneng.2019.106649>
- [4] Lee, G. N., Jung, K. H., Shin, S. Y., Park, H. J., Malenica, S., Chung, Y. S., Suh, S. B., 2022. Experimental study of green water on rectangular structure with varying flare angle. *Ocean Engineering*, 243, 110252. <https://doi.org/10.1016/j.oceaneng.2021.110252>
- [5] Oumeraci, H., Kortenhaus, A., Allsop, W., de Groot, M., Crouch, R., Vrijling, H., Voortman, H., 2001. Probabilistic design tools for vertical breakwaters. *CRC Press*.
- [6] DNV-RP-C205, 2010. Environmental Conditions and Environmental Loads.
- [7] Wagner, H., 1932. Über stoß-und gleitvorgänge an der oberfläche von flüssigkeiten. *ZAMM-Journal of Applied Mathematics and Mechanics/Zeitschrift für Angewandte Mathematik und Mechanik*, 12(4), 193-215. <https://doi.org/10.1002/zamm.19320120402>
- [8] Bullock, G., Bredmose, H., 2010. Breaking wave impacts on coastal structures. *In proceedings of the 5th Annual Conference on Advances in Computing and Technology*, January 25-29, London, UK.
- [9] Cuomo, G., Allsop, W., Bruce, T., Pearson, J., 2010. Breaking wave loads at vertical seawalls and breakwaters. *Coastal Engineering*, 57(4), 424-439. <https://doi.org/10.1016/j.coastaleng.2009.11.005>
- [10] Allsop, N. W. H., Vicinanza, D., McKenna, J. E., 1996. Wave forces on vertical and composite breakwaters. Report SR 443, *Hydraulics Research*, Wallingford, United Kingdom.
- [11] Ariyaratne, K., Chang, K. A., Mercier, R., 2012. Green water impact pressure on a three-dimensional model structure. *Experiments in Fluids*, 53 (6), 1879-1894. <https://doi.org/10.1007/s00348-012-1399-9>
- [12] Biggs, J. M., 1964. Introduction to structural dynamics. *McGraw-Hill Book Company*.
- [13] Seo, D., Jeong, K. L., 2019. Numerical study on the prediction of the bow flare slamming pressure for the container ship in regular wave. *Brodogradnja*, 70(1), 25-42. <https://doi.org/10.21278/brod70103>
- [14] Chopra, A. K., 2007. Dynamics of structures. *Pearson Education India*.
- [15] NORSOK N003, 1999. Actions and action effects. Norwegian Standards, Norway.
- [16] Hussein, A. W., Soares, C. G., 2009. Reliability and residual strength of double hull tankers designed according to the new IACS common structural rules. *Ocean Engineering*, 36(17-18), 1446-1459. <https://doi.org/10.1016/j.oceaneng.2009.04.006>

- [17] Hayashi, T., Tanaka, Y., 1988. Impact engineering. *Nikkan Kogyo Simbunsha (Daily Engineering Newspaper Company)*.
- [18] Zhu, L., Duan, L., Chen, M., Yu, T. X., Pedersen, P. T., 2020. Equivalent design pressure for ship plates subjected to moving slamming impact loads. *Marine Structures*, 71, 102741. <https://doi.org/10.1016/j.marstruc.2020.102741>
- [19] Wang, M., Qiao, D., Zhou, X., Tang, G., Lu, L., Ou, J., 2024. Dynamic responses analysis of submerged floating tunnel under impact load. *Brodogradnja*, 75(2), 75208. <https://doi.org/10.21278/brod75208>
- [20] Tu, J., Feng, F., Lu, Y., Wang, S., Cao, Q., 2025. Structural strength evaluation of a planing hull based on a one-way coupled CFD-FEA. *Brodogradnja*, 76(4), 76407. <https://doi.org/10.21278/brod76407>
- [21] Jiao, J., Chen, Z., Xu, S., 2024. CFD-FEM simulation of water entry of aluminium flat stiffened plate structure considering the effects of hydroelasticity. *Brodogradnja*, 75(1), 75108. <https://doi.org/10.21278/brod75108>
- [22] Leissa, A. W., 1969. Vibration of plates (Vol. 160). *Scientific and Technical Information Division, National Aeronautics and Space Administration*.
- [23] Lee, G. N., Jung, K. H., Chae, Y. J., Park, I. R., Malenica, S., Chung, Y. S., 2016. Experimental and numerical study of the behaviour and flow kinematics of the formation of green water on a rectangular structure. *Brodogradnja*, 67(3), 133-145. <https://doi.org/10.21278/brod67308>
- [24] Lee, G. N., 2020. Study of green water phenomena on rectangular structure. *Pusan National University*.
- [25] Cuomo, G., Allsop, W., Takahashi, S., 2010. Scaling wave impact pressures on vertical walls. *Coastal Engineering*, 57, 604-609. <https://doi.org/10.1016/j.coastaleng.2010.01.004>
- [26] Lin, S. M., Chuang, W. L., 2026. Experimental investigation of impact pressures and air entrainment effects during flat plate water entry at varying impact speeds and aeration levels. *Ocean Engineering*, 348, 124027. <https://doi.org/10.1016/j.oceaneng.2025.124027>
- [27] Takahashi, S., Tanimoto, K., Miyanaga, S., 1985. Uplift wave forces due to compression of enclosed air layer and their similitude law. *Coastal Engineering Japan*, 28, 191-206. <https://doi.org/10.1080/05785634.1985.11924415>
- [28] Ma, Z., Causon, D., Qian, L., Mingham, C., Mai, T., Greaves, D., Raby, A., 2016. Pure and aerated water entry of a flat plate. *Physics of Fluids*, 28(1), 016104. <https://doi.org/10.1063/1.4940043>
- [29] Bullock, G., Crawford, A., Hewson, P., Walkden, M., Bird, P., 2001. The influence of air and scale on wave impact pressures. *Coastal Engineering*, 42(4), 291-312. [https://doi.org/10.1016/S0378-3839\(00\)00065-X](https://doi.org/10.1016/S0378-3839(00)00065-X)
- [30] Harris, F. J. (2005). On the use of windows for harmonic analysis with the discrete Fourier transform. *Proceedings of the IEEE*, 66(1), 51-83. <https://doi.org/10.1109/PROC.1978.10837>
- [31] Park, D. M., Park, B., Lee, K., 2024. An Experimental Study of Wave Impact Loads on an FPSO Bow in 2D Wave-Tank. *Journal of Ocean Engineering and Technology*, 38(5), 218-231. <https://doi.org/10.26748/KSOE.2024.054>
- [32] Kudupudi, R. B., Bhattacharyya, A., Datta, R., 2020. A parametric study of green water impact on a container ship. *Ships and Offshore Structures*, 15(3), 318-324. <https://doi.org/10.1080/17445302.2019.1615728>
- [33] Jones, N., 2011. Structural impact. *Cambridge university press*. <https://doi.org/10.1017/CBO9780511820625>